Optimization of High-Yield Biological Synthesis of Single-Crystalline Gold Nanoplates

B. Liu,[†] J. Xie,[†] J. Y. Lee,*[,†,‡] Y. P Ting,[‡] and J. Paul Chen[‡]

Singapore−MIT Alliance, and Department of Chemical & Biomolecular Engineering, National University of Singapore, 10 Kent Ridge Crescent, Singapore 119260

Received: March 21, 2005; In Final Form: June 21, 2005

In this work, single-crystalline gold nanoplates were obtained by reducing aqueous chloroauric acid solution with the extract of *Sargassum sp*. (brown seaweed) at room temperature. The gold nanoplates so obtained were characterized by UV−vis spectroscopy, X-ray diffraction, atomic force microscopy, and transmission electron microscopy. The formation of gold nanoplates was found to depend on a number of environmental factors, such as the time taken to age the seaweed extract, pH of the reaction medium, reaction temperature, reaction time, and initial reactant concentrations. The size of the gold nanoplates could be controlled to between 200 and 800 nm by manipulating the initial reactant concentrations. The yield of the flat gold nanocrystals relative to the total number of nanoparticles formed was as high as ∼80−90%.

Introduction

The synthesis of metal nanoparticles with controlled chemical composition, size, and shape distributions is an important first step toward the realization of nanotechnology. Size and shape are pivotal in determining the physical and chemical properties of materials on the nanoscale.[1] The synthesis of metal nanoparticles with well-defined size and shape can be classified broadly into wet and dry methods. Wet methods often require the use of an aggressive chemical reducing agent such as sodium borohydride, hydroxylamine, or tetrakishydroxymethylphosphonium chloride (THPC),[2] a capping agent such as trioctyl phosphine oxide (TOPO),[3] and may additionally involve an organic solvent such as toluene or chloroform.[4] Dry methods, on the other hand, generate nanoparticles by ultraviolet irradiation, aerosol technology, or physical deposition into a solid template.[5] Although these methods may successfully produce pure, well-defined metal nanoparticles, the cost of production is relatively high both materially and environmentally. There is hence an unequivocal need to develop more cost-effective and environmental benign ("green chemistry") alternatives to these existing methods.[6] The choice of an environmentally compatible solvent system, an eco-friendly reducing agent, and a nonhazardous capping agent for the stabilization of the nanoparticles are three main criteria for a totally "green" nanoparticle synthesis. For these reasons researchers in the field of nanoparticle synthesis turn to the biological systems where many organisms, both unicellular and multicellular, are known to produce inorganic nanostructures either intracellularly[7] or extracellularly,[8] even though the actual mechanisms are not yet known because of the complexity of most biological reactions. Bacteria, yeasts, and fungi have been used to fabricate silver and gold nanoparticles.[9−11] While the intracellular synthesis in principle may accomplish a better control over the size and shape distributions of the nanoparticles, product harvesting, and recovery are more cumbersome and expensive. In addition, only a few types of nanoparticles of biological significance to the cellular organisms can be produced intracellularly. The extracellular synthesis by comparison is more adaptable to the synthesis of a wider range of nanoparticle systems.

Among various metal nanoparticles, gold nanoparticles are of particular interest to applications that leverage on their strongly size- and shape-dependent properties.[12] Hence, it is highly desirable to be able to produce gold nanoparticles with different morphology and size at high yields. Although there has been a large volume of work on the synthesis of gold nanoparticles and nanorods,[1g,2,4] there are relatively fewer attempts to produce gold nanoplates.[13−18] Among the few published successful efforts, either a complex multistep chemical process was involved[13] or the yield of the nanoplates relative to the total number of nanoparticles formed was low.[14−16] More recently, a wet chemistry route to scaling-up the production of micrometer-scale single-crystalline gold plates has been reported.[17] However, the lateral size and the thickness of the plates were relatively large and could not be easily manipulated by controlling the reaction conditions. Very recently, Sastry and co-workers developed a biological method to produce gold nanoprisms at 50% yield by using the extract of lemongrass leaves as a reducing agent cum shape-directing agent.[18] Since boiling was used to release the biochemical molecules in a noncontrollable manner, the analysis of the system response and process optimization are a daunting task. This study reports a simple biological synthesis of large quantities of gold nanoplates using a single step, room-temperature reduction of aqueous chloroaurate ions ($AuCl_4^-$) by seaweed extract. The yield of the gold nanoplates was remarkably high, at ∼80−90%, and the lateral size of the nanoplates could be controlled in the range of 200−800 nm. Experimental conditions such as the aging time of the seaweed extract, pH of the reaction medium, reaction temperature, reaction time, and initial reactant concentrations, were systematically varied to arrive at the optimal growth conditions for the gold nanoplates.

Experimental Section

Materials Preparation. *Sargassum sp.* belonging to the Phaeophyta division was collected from the west coast of Singapore and carefully washed with deionized water and dried

* To whom correspondence should be addressed. Email: cheleejy@nus.edu.sg.
[†] Singapore−MIT Alliance.
[‡] National University of Singapore.

10.1021/jp051449n CCC: $30.25
Published on Web 07/23/2005

naturally at room temperature. The dried seaweed was ground to a fine powder 0.5−1 mm in particle size. Prior to the experiments, the seaweed powder was washed several times with dilute HCl and deionized water to remove adsorbed impurities that might interfere with the formation of gold nanoparticles. About 1.0−2.0 g of thoroughly washed seaweed powder was added to 100 mL of deionized water and the mixture was aged for 1 to more than 10 days. In a typical experiment, 5−10 mL of this extract was mixed with 0−5 mL of deionized water, followed by the immediate addition of 1−2 mL of 0.01 M $HAuCl_4$ solution. The pH of the reaction medium was adjusted by adding 1 M NaOH solution or 1 M HCl solution. The reaction was carried out under vigorous stirring at room temperature or at elevated temperatures (vide infra) for 0−48 h.

Materials Characterization. (1) UV−Vis Measurements. UV−vis spectroscopy was carried out on a Shimadzu UV-3101 PC scanning spectrometer using deionized water as the reference. Two to three drops of the sample solution was pipetted into a quartz UV cell (2 mL) and diluted with deionized water, followed by immediate spectral measurements.

(2) TEM Measurements. Examination of the nanoparticle morphology by high-resolution analytical transmission electron microscopy (TEM) was performed on a JEM-2010 with an electron kinetic energy of 200 kV. For sample preparation, ∼2−3 drops of the colloidal gold solution were dispensed onto a carbon-coated 200-mesh copper grid and dried under ambient condition before examination.

(3) XRD Measurements. Crystallographic information about the samples was obtained from powder X-ray diffraction (XRD). XRD patterns were recorded by a Shimadzu X-ray diffractometer (Model 6000)[19] with Cu Kα radiation ($\lambda = 1.5406$ Å) scanning the 2θ range of 30−80° at 2° min^{-1}. The X-ray tube voltage and current were set at 40 kV and 30 mA, respectively.

(4) AFM Measurements. Surface topography and thickness of the samples were examined by atomic force microscopy (AFM; DI NanoScope MultiMode) in the tapping mode to minimize damage to the surface structures. A single-crystal silicon probe was used for the measurements. On the average, AFM images from more than three sampling locations per sample were recorded to ensure a good representation of the surface topography and thickness.

(5) Fourier Transform Infrared (FTIR) Spectroscopy. The chemical composition of the seaweed was characterized by FTIR (Bio-Rad) using the potassium bromide (KBr) pellet technique. About 2 mg of seaweed powder was mixed with approximately 100 mg of KBr to form the KBr pellet.

Results and Discussion

The seaweed used in this study was *Sargassum sp*., a brown alga (Figure SI-1) that has been characterized in a previous study.[20] It contains various sugars, mannitol, proteins, amino acids, cellulose, lipids, pigments, vitamins, and inorganic salts of primarily Na^+, K^+, Ca^{2+}, and Mg^{2+}.[21] The presence of the carboxylic, amine, phosphate, hydroxyl, and sulfhydryl functional groups[22] was confirmed by FTIR measurements (results not shown). The carbonyl, hydroxyl, and amine functional groups and tannic materials have the potential for metal ion reduction and for capping the nascently formed nanoparticles. These useful components for nanoparticle synthesis are easily leached out from the seaweed biomass because the high osmotic pressure within these halophiles causes a net diffusion of water into the protoplast when suspended in deionized water. In such a hypotonic environment, the protoplast swells before bursting and releasing the biomolecules.

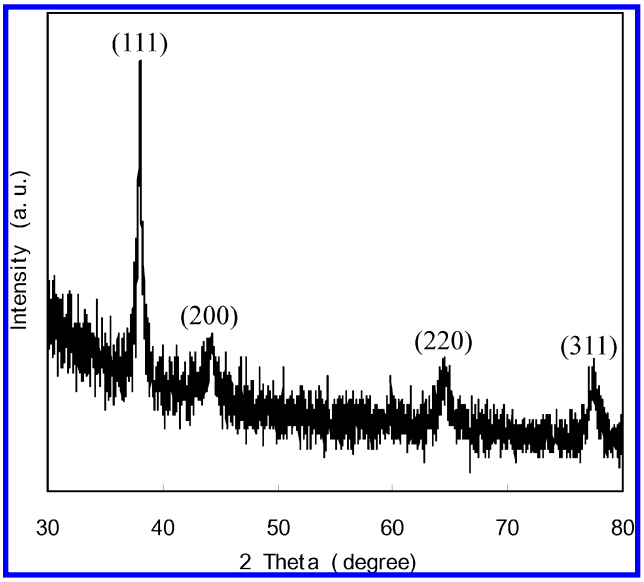

Figure 1. A representative XRD pattern of gold nanoplates synthesized by seaweed extract reduction of aqueous $AuCl_4^-$. Synthesis conditions: 5 of mL 5-day aged seaweed extract + 5 mL of deionized water + 1 mL of 0.01 M $HAuCl_4$ solution, neutral pH, room temperature for 5 h.

The seaweed extract used was a sticky light-yellow liquid, whose color was similar to that of the chloroauric acid solution. There was no color change upon mixing the chloroauric acid solution with the seaweed extract, although the color gradually changed with time. The color of the mixture after 0.5−1 h was slightly pinkish and became progressively darker with time (up to 3 h). Such color changes are usually indicative of changes in the metal oxidation state. In this case, Au(III) was reduced to Au(0) by some yet to be identified biomolecules in the seaweed extract.

Figure 1 shows a representative XRD pattern of the gold nanoplates synthesized by the seaweed extract. A number of Bragg reflections were present which could be indexed on the basis of the face-centered cubic (fcc) gold structure. No spurious diffractions due to crystallographic impurities were found. The XRD pattern clearly shows that the gold nanoplates were crystalline. In addition, the intensity of the (111) diffraction was much stronger than those of the (200) and (220) diffractions. These observations indicate that the gold nanoplates formed by the reduction of Au(III) by seaweed extract were dominated by {111} facets, and hence more {111} planes parallel to the surface of the supporting substrate were sampled.

A typical TEM image showing the size and morphology of the gold nanoplates is given in Figure 2. The nanoplates, which were 300−400 nm in size along their longest edge and 8−10 nm in thickness (corroborated by AFM measurements), were of hexagonal, truncated triangular, and triangular geometries with very smooth edges. Continuous and randomly distributed pairs of bending contours, which are frequently encountered in the bright-field TEM image of nanobelts, can be found across the flat crystal faces. The bending contours are caused by the warping of the atomic planes with respect to the direction of the incident electron beam.[23] The single-crystalline structure of these nanoplates was further confirmed by their corresponding electron diffraction patterns. Parts C and D of Figure 2 show the TEM image of an isolated nanoplate and its corresponding selected-area electron diffraction (SAED) pattern. The SAED pattern was obtained by aligning the electron beam perpendicular

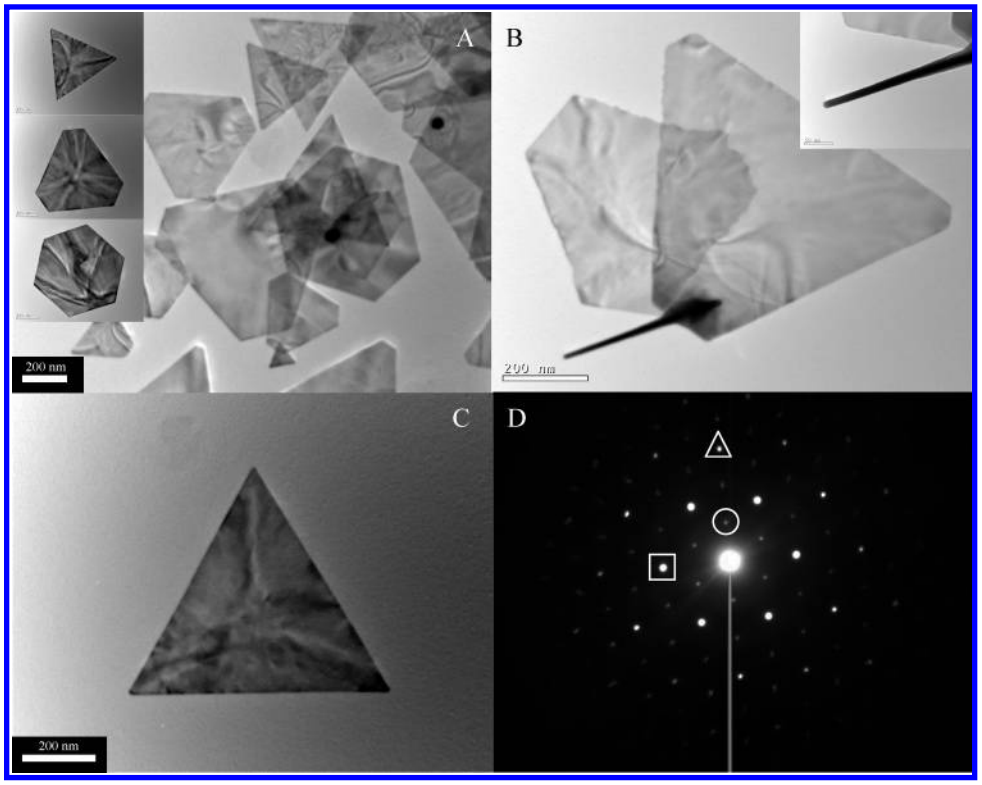

Figure 2. (A and B) Representative TEM images of gold nanoplates synthesized by the reduction of aqueous $AuCl_4^-$ by seaweed extract. The inset in (A) shows three types of gold nanoplates: triangular, truncated triangular, and hexagonal. The inset in (B) shows a gold nanoplate standing perpendicular to the TEM grid, which allows the precise measurement of its thickness. (C and D) An enlarged TEM image of a triangular gold nanoplate and its corresponding SAED pattern. The strongest spots (squares) could be indexed to the {220} reflections, the outer spots (triangles) with weaker intensity could be assigned to the {422} reflections, and the inner spots (circles) with the weakest intensity correspond to the formally forbidden $^1/_3${422} reflections. Synthesis conditions: (A and C) 5 mL of 5-day aged seaweed extract + 5 mL of deionized water + 1 mL of 0.01 M $HAuCl_4$ solution, neutral pH, room temperature for 5 h; (B) 5 mL of 5-day aged seaweed extract + 5 mL of deionized water + 1 mL of 0.01 M $HAuCl_4$ solution, neutral pH, room temperature for 2 h.

to the triangular facet of the nanoplate. The hexagonal symmetry of the diffracted spots suggests that each gold nanoplate was a single crystal bounded by triangular {111} facets. Three sets of spots could be identified from this diffraction pattern: the set with the strongest intensity could be indexed to the {220} planes of fcc gold. The outer set with a weaker intensity was caused by reflections from the {422} planes. The inner set with the weakest intensity corresponds to the formally forbidden $^1/_3${422} reflections. All these observations are consistent with previous studies on gold (or silver) nanocrystals bounded by atomically flat surfaces.[1c,1d]

It is well known that the optical properties of metal nanoparticles are strongly size and shape dependent. The anisotropy in the gold nanoplate geometry matters most to optical properties related to light absorption, scattering, and surface enhanced Raman effects. According to the Mie theory,[24] small spherical nanocrystals (either Ag or Au) should exhibit only a single surface plasmon resonance (SPR), whereas anisotropic particles would have two to three SPR bands, depending on their shape. Larger particles can also display additional bands arising from quadrupole and higher multipole plasmon excitations.[1c] Figure 3 shows a typical UV−vis spectrum of gold nanoplates obtained by reducing chloroauric ions with a seaweed extract that had been aged for 7 days. Two broad SPR bands centering at 525 and 1015 nm are clearly visible, which could be attributed to the in-plane dipole resonance and the out-of-plane quadrupole resonance, respectively.[1c,12c] It has been reported that the in-plane dipole plasmon absorption peak is highly sensitive to the sharpness of the triangle vertexes.[1c] As there existed three types of nanoplates: hexagonal, truncated triangular, and triangular;

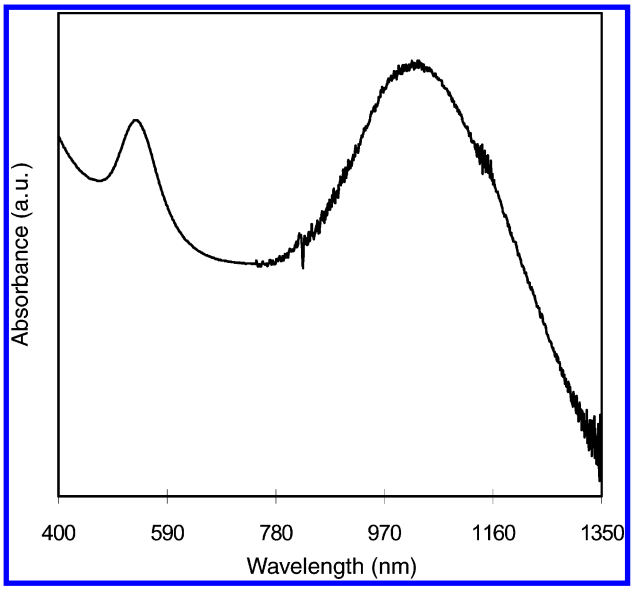

Figure 3. UV−vis spectrum of gold nanoplates synthesized by reducing chloroaurate ions with seaweed extract. Synthesis conditions: 5 mL of 7-day aged seaweed extract + 5 mL of deionized water + 1 mL of 0.01 M $HAuCl_4$ solution, neutral pH, room temperature for 3 h.

the in-plane dipole plasmon absorption band of our sample was naturally broadened.

When seaweed powder instead of seaweed extract for the reduction of chloroaurate anions, gold nanoparticles measuring 5−10 nm in diameters were produced without any trace of hexagonal or triangular nanoplates (see Figure SI-2). The

TABLE 1: Summary of Experimental Variables and Product Morphologies

experimental variables		product morphology
pH[a]	1	no product
	4	no product
	7	plates
	10	particles
	13	particles
reaction temperature[b] (°C)	room temperature	plates
	70	interrupted plates and particles
	90	interrupted plates and particles
	180	particles
	>250	no product
aging time of seaweed extract[c] (day)	1	plates
	3	plates
	7	plates
	>10	plates and particles
reactant concentrations[d]	10 + 0 + 1	plates
	5 + 5 + 1	plates
	5 + 5 + 2	plates
reaction time[e] (h)	1	corrugated plates
	3	plates
	5	plates
	24	plates
	48	plates and particles

[a] 5 mL of 1-day aged seaweed extract + 5 mL of deionized water + 1 mL of 0.01 M $HAuCl_4$ solution, room temperature for 3 h under different initial pH. [b] 5 mL of 3-day aged seaweed extract + 5 mL of deionized water + 1 mL of 0.01 M $HAuCl_4$ solution, neutral pH for 3 h at different reaction temperature. [c] 5 mL of seaweed extract (aged for different periods of time) + 5 mL of deionized water + 1 mL of 0.01 M $HAuCl_4$ solution, neutral pH, room temperature for 3 h. [d] 10 mL of 5-day aged seaweed extract + 1 mL of 0.01 M $HAuCl_4$ solution, neutral pH, room temperature for 3 h; 5 mL of seaweed 5-day aged extract + 5 mL of deionized water + 1 mL of 0.01 M $HAuCl_4$ solution, neutral pH, room temperature for 3 h and 5 mL of 5-day aged seaweed extract + 5 mL of deionized water + 2 mL of 0.01 M $HAuCl_4$ solution, neutral pH, room temperature for 3 h. [e] 10 mL of 5-day aged seaweed extract + 1 mL of 0.01 M $HAuCl_4$ solution, neutral pH, room temperature for different reaction time.

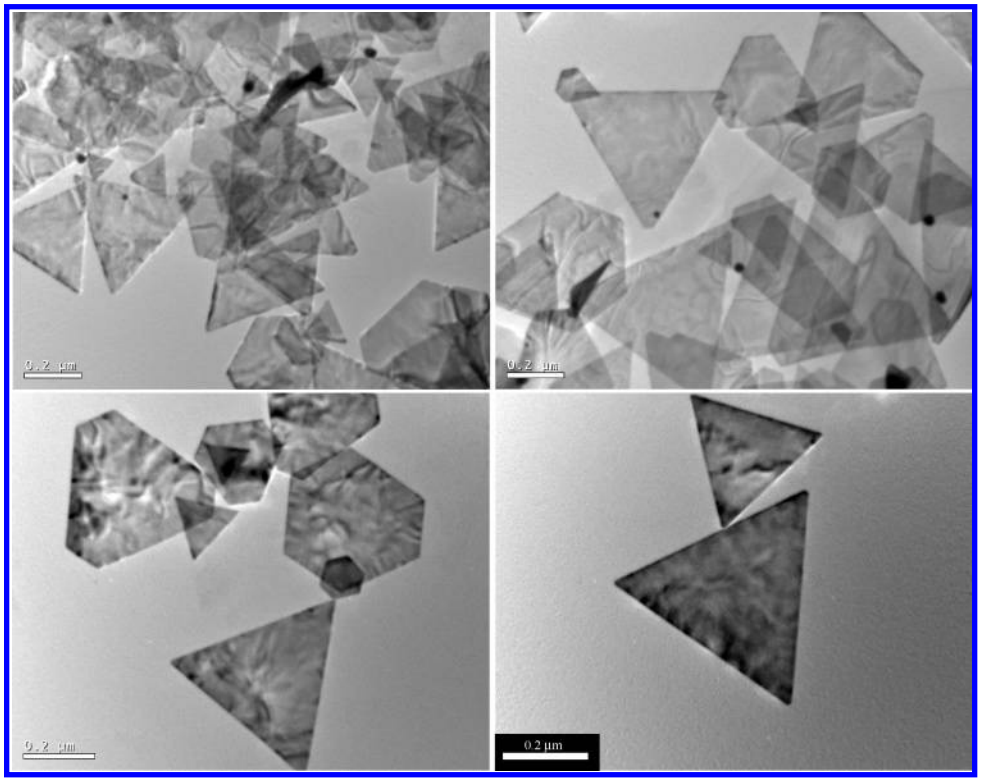

Figure 4. TEM images of gold nanoplates synthesized under neutral pH. Synthesis conditions: 5 mL of 1-day aged seaweed extract + 5 mL of deionized water + 1 mL of 0.01 M $HAuCl_4$ solution, neutral pH, room temperature for 3 h.

experimentally observed kinetics led to the following hypothesis: It is postulated that the seaweed biomass provided both the reducing agent(s) (R) and the capping agents (A and B) necessary for the gold nanoplate synthesis from its repertoire of functional biochemicals. The capping agents may be further divided into two classes. One assisted to limit the size (A) and the other assisted to control the shape (B). Hence A would bind nonspecifically on all exposed surfaces of gold whereas the binding of B was stronger on certain facets of gold. The diffusion of R, A, and B from the seaweed biomass to the aqueous solution occurred at different rates because of the difference in size and structures of these molecules of biological origin. It is further hypothesized that the diffusion of the shape-controlling agent B was the slowest. When seaweed powder

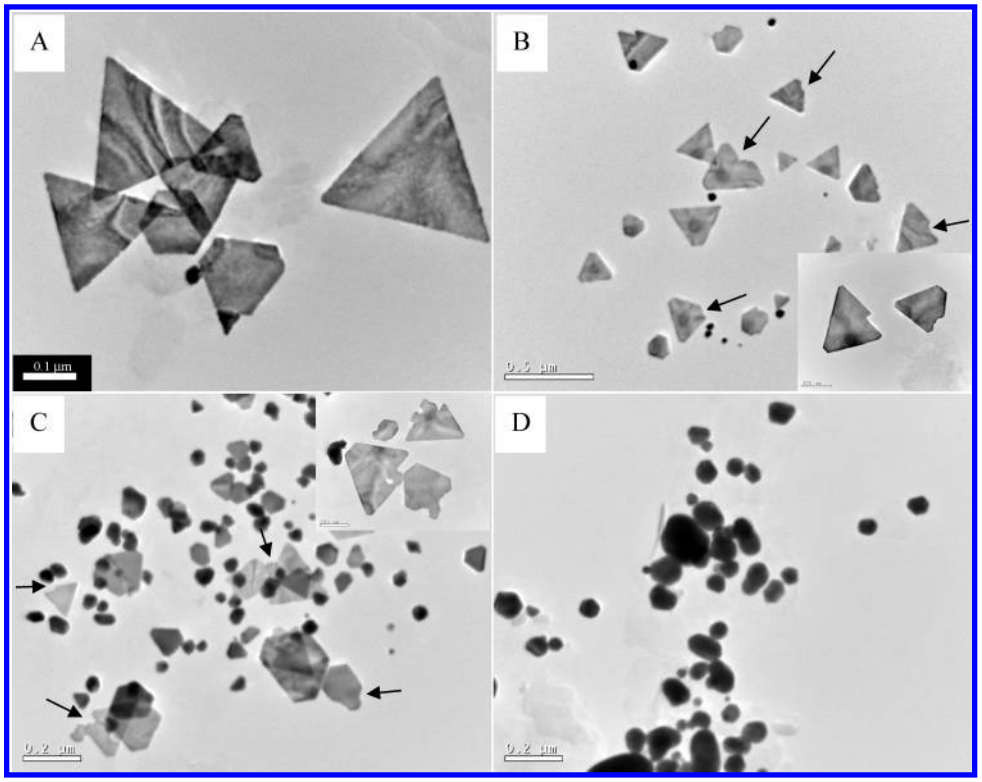

Figure 5. TEM images of gold nanoplates synthesized at different reaction temperatures. Synthesis conditions: 5 mL of 3-day aged seaweed extract + 5 mL of deionized water + 1 mL of 0.01 M $HAuCl_4$ solution, neutral pH, 3 h of reaction at (A) room-temperature, (B) 70 °C, (C) 90 °C, and (D) 180 °C. Arrows indicate the presence of interrupted gold nanoplates. Insets are high-magnification TEM images.

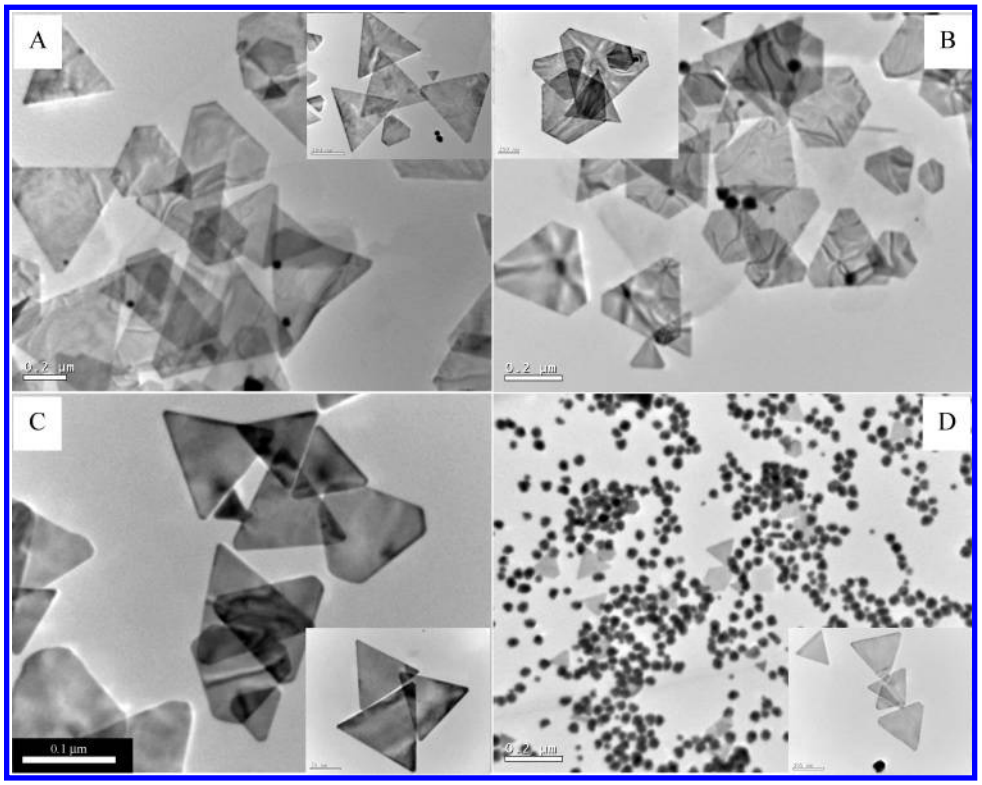

Figure 6. TEM images of gold nanoplates synthesized by seaweed extract aged for different periods of time. Synthesis conditions: 5 mL of seaweed extract + 5 mL of deionized water + 1 mL of 0.01 M $HAuCl_4$ solution, neutral pH, room temperature for 3 h. The seaweed extract was aged for (A) 1 day, (B) 3 days, (C) 7 days, and (D) more than 10 days. Insets are high-magnification TEM images.

was mixed with aqueous chloroauric acid directly, large quantities of R and A were released without B within a relatively short period of time. The relatively fast reduction reaction (the solution changed color from pale yellow to pink within 1 h) was therefore conducted in the absence or insufficient presence of the shape-controlling agent B. Consequently the gold nanoparticles grew without any shape control. Further, the size of the nanoparticles formed was kept small by the abundant presence of A in the solution. On the other hand, the concentration of B in a sufficiently aged seaweed extract would be high

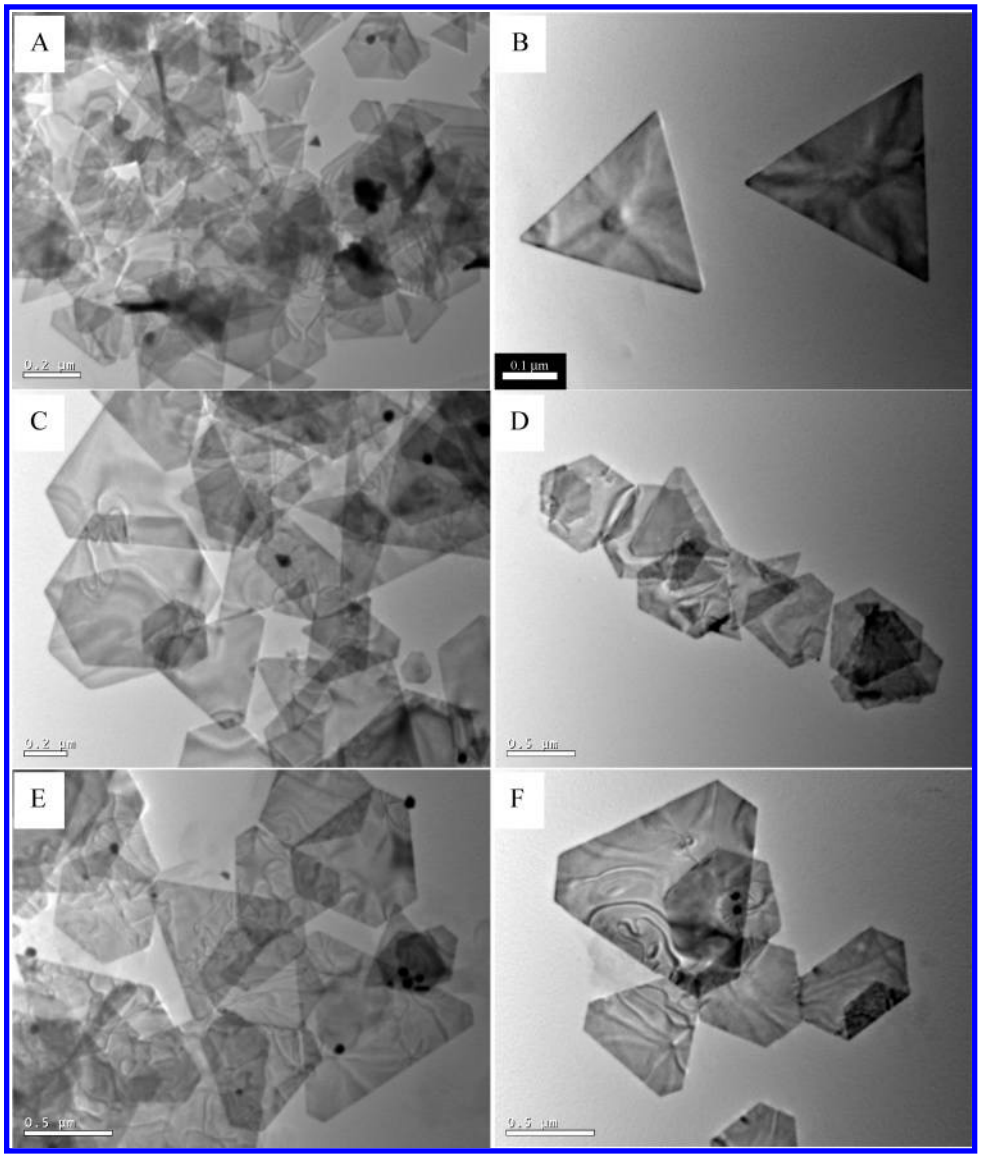

Figure 7. TEM images of gold nanoplates synthesized by reactants of different concentrations. Synthesis conditions: (A and B) 10 mL of 5-day aged seaweed extract + 1 mL of 0.01 M $HAuCl_4$ solution, neutral pH, room temperature for 3 h. (C and D) 5 mL of 5-day aged seaweed extract + 5 mL of deionized water + 1 mL of 0.01 M $HAuCl_4$ solution, neutral pH, room temperature for 3 h. (E and F) 5 mL of 5-day aged seaweed extract + 5 mL of deionized water + 2 mL of 0.01 M $HAuCl_4$ solution, neutral pH, room temperature for 3 h.

enough to exercise shape control. The formation of platelike gold nanostructures was initiated by the adsorption of the shape-controlling agent B on the selected facets of gold nuclei formed in the reduction process. Different crystal facets are expected to exhibit different adsorptivities for B, but the strongly adsorbed surfaces were hindered in their continuing growth. The facets with fewer attached capping molecules would then grow more rapidly relative to the others. As a result, a specific shape was formed. In the current case, the shape-controlling capping agent B was preferentially adsorbed on the {111} facets and suppressed the growth in the ⟨111⟩ direction. Thus, anisotropic polygonal plates covered by {111} facets were formed.

Environmental factors in the synthesis, such as pH, reaction temperature, aging time of the seaweed extract, initial reactant concentrations, and reaction time, could affect the release and maintenance of these biologically derived reducing and capping agents and hence the yield and quality of the gold nanoplates. A series of experiments was therefore carried out to examine the effects of these preparative parameters. The results are summarized in Table 1.

Effect of pH. The formation of gold nanoplates was most favored under neutral pH. The lateral size of the nanoplates produced was around 200−300 nm (Figure 4). At lower pH, no product was formed in the solution even after reaction up to a day (based on UV/visible spectroscopic measurements, Figure SI-3). In alkaline solutions only nanoparticles were produced. The size of the nanoparticles formed at pH = 10 was in the range of 5−10 nm. Further increase in initial pH to 13 led to the formation of irregularly shaped particles 300−500 nm in diameter (see Figure SI-4) most probably as hydrated gold oxides.[25]

Effect of Reaction Temperature. Figure 5 shows the effect of reaction temperature on gold nanoplate formation. Well-defined hexagonal, truncated triangular, and triangular gold nanoplates were produced at room temperature. The nanoplates all had very smooth edges and sharp vertexes. Increase in reaction temperature caused the formation of interrupted gold nanoplates (shown by arrows in Figure 5) accompanied by an increasing number of larger nanoparticles. However, no solid product was formed when the temperature was raised to 250

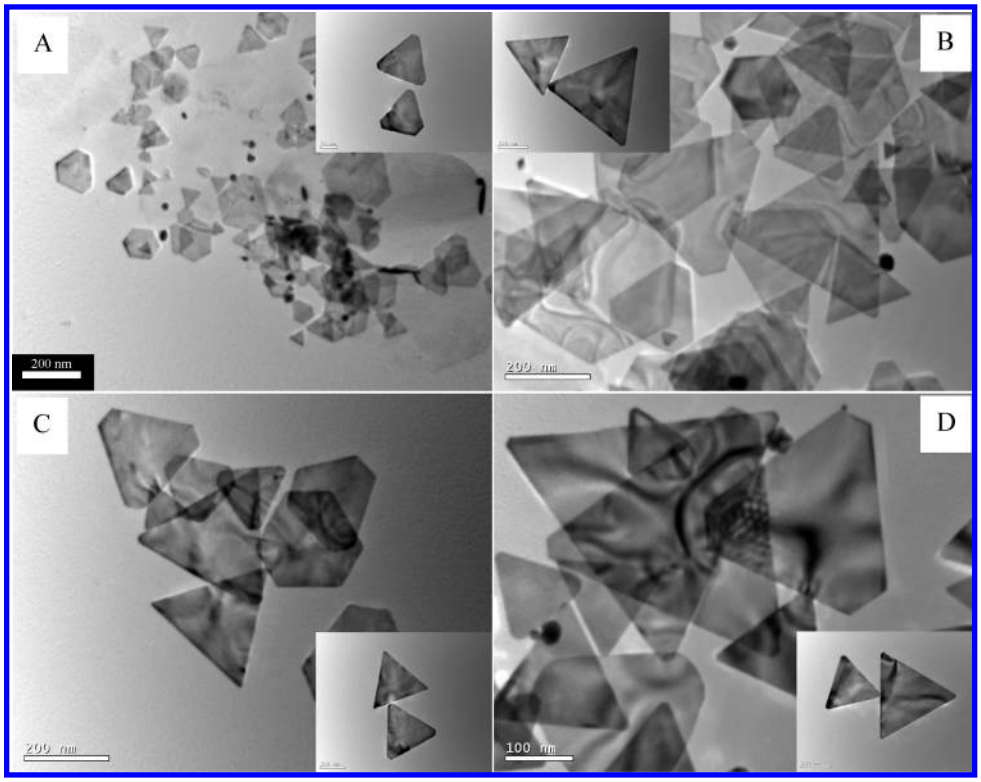

Figure 8. TEM images of gold nanoplates synthesized at different reaction times. Synthesis conditions: 10 mL of 5-day aged seaweed extract + 1 mL of 0.01 M $HAuCl_4$ solution, neutral pH, room temperature. (A) 1 h, (B) 3 h, (C) 5 h, and (D) 24 h. Insets are high-magnification TEM images.

°C (under hydrothermal condition in a Teflon-lined stainless steel autoclave). UV−vis spectroscopy (not shown) of the reaction mixture then showed only the absorption band due to $HAuCl_4$ at 300 nm, indicating no reduction was possible at 250 °C and beyond. This can be understood by the biological origin of the reducing and capping agents which are easily degraded by temperature increase (to various degrees) and accelerated nucleation at higher temperatures. The formation of interrupted nanoplates (at slightly elevated temperatures) was mechanistically similar to the formation of corrugated nanoplates at the very early stage of the reaction (vide infra).

Effect of Aging Time of Seaweed Extract. It is shown in Figure 6 that an increase in the aging time of seaweed extract favored the formation of smaller gold nanoplates. A seaweed extract that had been aged for 1 day produced gold nanoplates 200−300 nm in size, and the size decreased to 150−200 nm and to 100−150 nm when a 3-day aged and a 7-day aged seaweed extract was used, respectively. Using a seaweed extract that had been aged for more than 10 days resulted in a small number of gold nanoplates among a large excess of gold nanoparticles 30−40 nm in diameters. This could be understood in terms of the competition between diffusive accumulation and denaturation of the capping agents. For short extraction times, the rate of diffusion of the capping agents was higher than the rate of their degradation, resulting in the accumulation of the capping agents in the extract, which directed the formation of gold nanoplates. At longer times, the rate of diffusion of the capping agents was reduced due to source depletion while the rate of degradation was either unchanged or increased depending on the reaction order of denaturation. There should exist a point in time when the rates of diffusion and degradation were in balance, beyond which the summed concentration of the available capping agents in the extract would decrease with aging time, leading to the loss of control for size and growth direction, and large (30−40 nm) gold nanoparticles were formed as a result. Another experiment was conducted to validate this hypothesis. In this experiment, a seaweed extract was obtained after 3 days of aging and was stored at room temperature for another 4 days before use. TEM examination showed the formation of a mixture of nanoplates and large nanoparticles (see Figure SI-5), which was in strong contrast to using a 3-day aged or a 7-day aged seaweed extract, where large quantities of gold nanoplates 150−200 or 100−150 nm in size were formed. In this experiment, a sufficient quantity of reducing and capping agents was accumulated after 3 days of aging. During the subsequent 4 days of storage in the absence of the seaweed biomass, there was no further supply of both the reducing and capping agents to the extract but the natural degradation of these biological components went unabated. The net result was a decrease in the concentrations of the reducing and capping agents, which prompted the formation of a mixture of nanoplates and larger nanoparticles 50−60 nm in size.

Effect of Initial Reactant Concentrations. The size of the gold nanoplates could be tuned in the range of 200−800 nm by manipulating the initial reactant concentrations (shown in Figure 7). Concentrated seaweed extract promoted the formation of smaller gold nanoplates. UV−vis measurements showed a slight shift in the Au SPR band for nanoplates with different sizes (see Figure SI-6).

Effect of Reaction Time. The kinetics of gold nanoplate formation in the $AuCl_4^-$−seaweed extract reaction was examined by varying the reaction time. At the very early stage of reaction (1 h, Figure 8A), flat particles with corrugated edges were formed instead of previously reported aggregates of particles in the size range of 0.3−5 μm.[18] SAED measurements of these corrugated nanoplates produced a series of hexagonal spots, indicating that these flat nanoplates were single crystals (data not shown). Between 3 and 24 h of reaction time, the size of the gold nanoplates grew while the edges became increasingly smoother. A number of nanoplates with peculiar morphologies were also formed at the same time (see Figure SI-7). On the basis of these observations, we postulate that the

growth of gold nanoplates in this biological synthesis followed the "surface wrapping" mechanism proposed by Zeng and coworkers[26] rather than the recently proposed self-assembly mechanism proposed.[18] The growth of gold nanoplates was very fast at the early stage of reaction. Once the wrapping layer was formed, it directed the growth of another layer, and steps and corrugated edges were formed as a result. With the increase in reaction time, the reaction rate was reduced because of reactant depletion, and the deposition of gold would then follow the most energetically favorable direction. The steps were leveled and the edges smoothened. In addition, the lack of significant growth in thickness was another evidence for the "surface wrapping" mechanism. When the reaction time was lengthened to 48 h, more nanoparticles were generated (results not shown) due to the depletion of the capping agents by consumption in the earlier reaction and also by denaturation.

While light irradiation is an essential condition for generating flat triangular silver nanoparticles,[1c,1d] it was inconsequential to the current biological synthesis. Well-defined gold nanoplates could also be produced in a dark reaction environment (see Figure SI-8). There were no significant differences between reactions carried out with or without light.

The chemical identities of the reducing agents (R) and capping agents (A and B) and the detailed mechanism for the formation of gold nanoplates by seaweed extract reduction of gold precursor salts are not understood at present. It is rather the purpose of this paper to demonstrate the power of biologically inspired synthesis and to mimic nature' way of maximizing effort at minimum cost. In a first attempt to obtain further insights about the reaction, we separated the seaweed extract into different fractions based on molecular weight (using 10k cutoff filters) and functional group (based on reverse-phase high-pressure liquid chromatography) differences. The preliminary results have implicated proteins as the major active species. The effects of amino acid sequence, size, shape, and charge of the proteins are still being investigated.

Conclusions

Hexagonal, truncated triangular, and triangular nanoplates of gold have been obtained by the reduction of chloroaurate anions in water by seaweed extract. The yield of flat gold nanocrystals relative to the total number of nanoparticle formed under neutral pH and room temperature was around ~80−90%, which is significantly higher than the current literature value of 50%. The formation of nanoplates was found to be affected by a number of factors such as pH of the reaction mixture, reaction temperature, aging time of the seaweed extract, initial reactant concentrations, and reaction time. In general, neutral pH and room temperature favored the formation of well-defined gold nanoplates. By simply varying the initial reactant concentrations, the size of the gold nanoplates could be controlled between 200 and 800 nm.

Acknowledgment. The present work is supported by Singapore−MIT Alliance. We are grateful to Prof. H. C. Zeng and Mr. L. Yang for their useful discussion.

Supporting Information Available: Pictures of fresh *Sargassum* sp., UV−vis spectra, and TEM images of gold nanoparticles obtained under intermediate conditions are available free of charge via the Internet at http://pubs.acs.org.

References and Notes

(1) (a) Li, L.; Alivisatos, A. P. *Nano Lett.* **2001**, *1*, 349. (b) Manna, L.; Scher, E. C.; Alivisatos, A. P. *J. Am. Chem. Soc.* **2000**, *122*, 12700. (c) Jin, R. C.; Cao, Y. W.; Mirkin, C. A.; Kelly, K. L.; Schatz, G. C.; Zheng, J. G. *Science* **2001**, *294*, 1901. (d) Jin, R. C.; Cao, Y. C.; Hao, E. C.; Métraux, G. S.; Schatz, G. C.; Mirkin, C. A. *Nature* **2003**, *425*, 487. (e) Sun, Y. G.; Xia, Y. N. *Anal. Chem.* **2003**, *128*, 686. (f) Kim, F.; Connor, S.; Song, H. J.; Kuykendall, T.; Yang, P. D. *Angew. Chem., Int. Ed.* **2004**, *43*, 3673. (g) Sau, T. K.; Murphy, C. J. *J. Am. Chem. Soc.* **2004**, *126*, 8648.

(2) (a) Gole, A.; Murphy, C. J. *Chem. Mater.* **2004**, *16*, 3633. (b) Gao, J.; Bender, C. M.; Murphy, C. J. *Langmuir* **2003**, *19*, 9065. (c) Jana, N. R.; Gearheart, L.; Murphy, C. J. *Langmuir* **2001**, *17*, 6782. (d) Jana, N. R.; Gearheart, L.; Murphy, C. J. *J. Phys. Chem. B* **2001**, *105*, 4065. (e) Koel, B. E.; Meltzer, S.; Resch, R.; Thompson, M. E.; Madhukar, A.; Requicha, A. A. G.; Will, P. *Langmuir* **2001**, *17*, 1713. (f) Halas, N. J.; Westcott, S. L.; Oldenburg, S. J.; Lee, T. R. *Langmuir* **1998**, *14*, 5396.

(3) (a) Puntes, V. F.; Krishnan, K. M.; Alivisatos, A. P. *Science* **2001**, *291*, 2115. (b) Peng, Z. A.; Peng, X. G. *J. Am. Chem. Soc.* **2002**, *124*, 3343.

(4) (a) Brust, M.; Walker, M.; Bethell, D.; Schiffrin, D. J.; Whyman, R. *J. Chem. Soc., Chem. Commun.* **1994**, 801. (b) Gittins, D. I.; Caruso, F. *Angew. Chem., Int. Ed.* **2001**, *40*, 3001. (c) Gittins, D. I.; Caruso, F. *ChemPhysChem* **2002**, *3*, 110. (d) Selvakannan, P. R.; Mandal, S.; Pasricha, R.; Adyanthaya, S. D.; Sastry, M. *Chem. Commun.* **2002**, *13*, 1334.

(5) (a) Chen, Z. Y.; Zhou, Y.; Wang, C. Y.; Zhu, Y. R. *Chem. Mater.* **1999**, *11*, 2310. (b) Magnusson, M. H.; Deppert, K.; Malm, J.; Bovin, J.; Samuelson, L. *Nanostruct. Mater.* **1999**, *12*, 45. (c) Magnusson, M. H.; Deppert, K.; Malm, J.; Bovin, J.; Samuelson, L. *J. Nanopart. Res.* **1999**, *1*, 243. (d) Tolles, W. M. *Nanotechnology* **1996**, *7*, 59.

(6) Raveendran, P.; Fu, J.; Wallen, S. L. *J. Am. Chem. Soc.* **2003**, *125*, 13940.

(7) (a) Gardea-Torresdey, J. L.; Parsons, J. G.; Gomez, E.; Peralta-Videa, J.; Troiani, H. E.; Santiago, P.; Yacaman, M. J. *Nano Lett.* **2002**, *2*, 397. (b) Mukherjee, P.; Ahmad, A.; Mandal, D.; Senapati, S.; Sainkar, R. S.; Khan, M. I.; Parishcha, R.; Ajaykumar, P. V.; Alam, M.; Kumar, R.; Sastry, M. *Nano Lett.* **2001**, *1*, 515. (c) Ahmad, A.; Senapati, S.; Khan, M. I.; Kumar, R.; Ramani, R.; Srinivas, V.; Sastry, M. *Nanotechnology* **2003**, *14*, 824.

(8) (a) Ahmad, A.; Senapati, S.; Khan, M. I.; Kumar, R.; Sastry, M. *Langmuir* **2003**, *19*, 3550. (b) Ahmad, A.; Mukherjee, P.; Senapati, S.; Mandal, D.; Khan, M. I.; Kumar, R.; Sastry, M. *Colloids Surf. B* **2003**, *28*, 313. (c) Ahmad, A.; Mukherjee, P.; Mandal, D.; Senapati, S.; Khan, M. I.; Kumar, R.; Sastry, M. *J. Am. Chem. Soc.* **2002**, *124*, 12108.

(9) Klaus, T.; Joerger, R.; Olsson, E.; Granqvist, C. G. *Proc. Natl. Acad. Sci. U.S.A.* **1999**, *96*, 13611.

(10) Kowshik, M.; Ashtaputre, S.; Kharrazi, S.; Vogel, W.; Urban, J.; Kulkarni, S. K.; Paknikar, K. M. *Nanotechnology* **2003**, *14*, 95.

(11) (a) Mukherjee, P.; Ahmad, A.; Mandal, D.; Senapati, S.; Sainkar, S. R.; Khan, M. I.; Ramani, R.; Parischa, R.; Ajayakumar, P. V.; Alam, M.; Sastry, M.; Kumar, R. *Angew. Chem., Int. Ed.* **2001**, *40*, 3585. (b) Mukherjee, P.; Senapati, S.; Mandal, D.; Ahmad, A.; Khan, M. I.; Kumar, R.; Sastry, M. *ChemBioChem* **2002**, *3*, 461.

(12) (a) Kim, F.; Song, J. H.; Yang, P. D. *J. Am. Chem. Soc.* **2002**, *124*, 14316. (b) Sun, Y. G.; Xia, Y. N. *Science* **2002**, *298*, 2176. (c) Hao, E. C.; Bailey, R. C.; Schatz, G. C.; Hupp, J. T.; Li, S. Y. *Nano Lett.* **2004**, *4*, 327. (d) Suzuki, M.; Niidome, Y.; Kuwahara, Y.; Terasaki, N.; Inoue, K.; Yamada, S. *J. Phys. Chem. B* **2004**, *108*, 11660.

(13) Kim, J. U.; Cha, S. H.; Shin, K.; Jho, J. Y.; Lee, J. C. *Adv. Mater.* **2004**, *16*, 459.

(14) Brown, S.; Sarikaya, M.; Johnson, E. *J. Mol. Biol.* **2000**, *299*, 725.

(15) Malikova, N.; Pastoriza-Santos, I.; Schierhorn, M.; Kotov, N. A.; Liz-Marzán, L. M. *Langmuir* **2002**, *18*, 3694.

(16) Shao, Y.; Jin, Y. D.; Dong, S. J. *Chem. Commun.* **2004**, *9*, 1104.

(17) Sun, X. P.; Dong, S. J.; Wang, E. K. *Angew. Chem., Int. Ed.* **2004**, *43*, 6360.

(18) Shankar, S. S.; Rai, A.; Ankamwar, B.; Singh, A.; Ahmad, A.; Sastry, M. *Nature Mater.* **2004**, *3*, 482.

(19) (a) Liu, B.; Zeng, H. C. *J. Am. Chem. Soc.* **2003**, *125*, 4430. (b) Liu, B.; Zeng, H. C. *J. Am. Chem. Soc.* **2004**, *126*, 8124. (c) Liu, B.; Zeng, H. C. *J. Am. Chem. Soc.* **2004**, *126*, 16744.

(20) Sheng, P. X.; Ting, Y. P.; Chen, J. P.; Hong, L. *J. Colloid Interface Sci.* **2004**, *275*, 131.

(21) Mautner, G. H. *Econ. Bot.* **1954**, *8*, 174.

(22) Crist, R. H.; Oberhosolar, K.; Shank, N.; Ngkuyen, M. *Environ. Sci. Technol.* **1981**, *15*, 1212.

(23) Ding, Y.; Wang, Z. L. *J. Phys. Chem. B* **2004**, *108*, 12280.

(24) Mie, G. *Ann. Phys.* **1908**, *25*, 377.

(25) *Advanced Inorganic Chemistry*; Cotton, F. A., Wilkinson, G., Murillo, C. A., Bochmann, M., Eds.; Wiley-Interscience: New York 1999, 1101.

(26) Feng, J.; Zeng, H. C. *Chem. Mater.* **2003**, *15*, 2829.